AD-A088 806 OHIO STATE UNIV COLUMBUS ELECTROSCIENCE LAB F/G 17/9
ON THE APPLICATION OF THE GTD-MM TECHNIQUE AND ITS LIMITATIONS,(U
JUL 80 J N SAHALOS, G A THIELE F19628-78-C-0198
UNCLASSIFIED ESL-711353-1 RADC-TR-80-14 NL

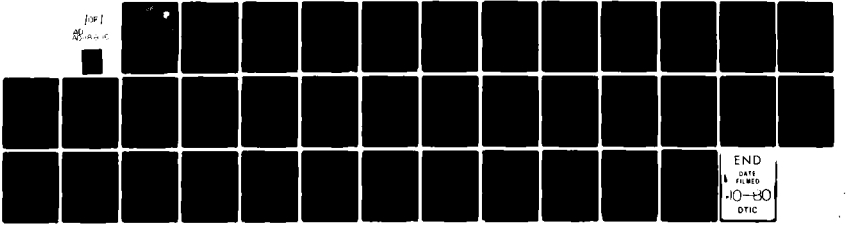

END
DATE FILMED
10-80
DTIC

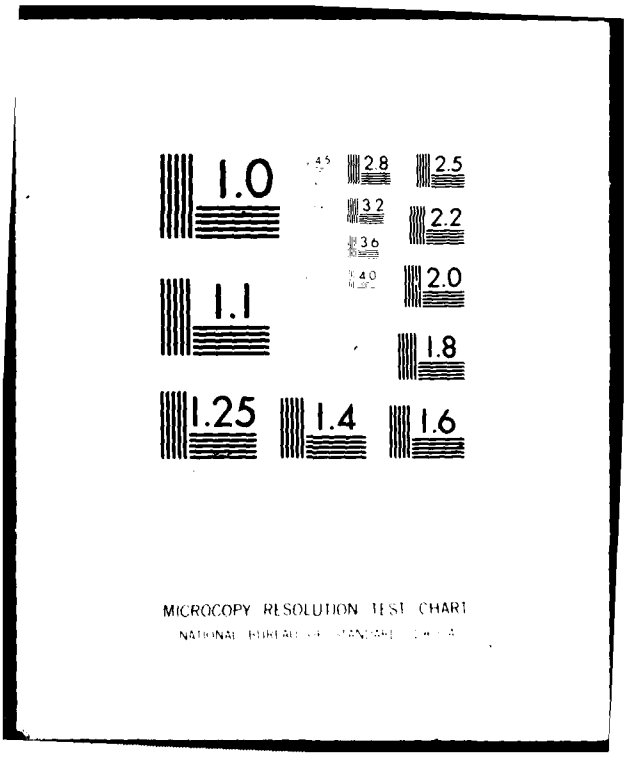
1.0
2.8
2.5
3.2
2.2
3.6
4.0
2.0
1.1
1.8
1.25
1.4
1.6
MICROCOPY RESOLUTION TEST CHART

LEVEL II

RADC-TR-80-14
Phase Report
July 1980

ON THE APPLICATION OF THE GTD-MM TECHNIQUE AND ITS LIMITATIONS

The Ohio State University of ElectroScience Laboratory

John N. Sahalos
Gary A. Thiele

ROME AIR DEVELOPMENT CENTER
Air Force Systems Command
Griffiss Air Force Base, New York 13441

This report has been reviewed by the RADC Public Affairs Office (PA) and is releasable to the National Technical Information Service (NTIS). At NTIS it will be releasable to the general public, including foreign nations.

RADC-TR-80-14 has been reviewed and is approved for publication.

APPROVED: Ronald G. Newburgh

RONALD G. NEWBURGH
Project Engineer

APPROVED: Allan C. Schell

ALLAN C. SCHELL
Chief, Electromagnetic Sciences Division

FOR THE COMMANDER: John P. Huss

JOHN P. HUSS
Acting Chief, Plans Office

SUBJECT TO EXPORT CONTROL LAWS

This document contains information for manufacturing or using munitions of war. Export of the information contained herein, or release to foreign nationals within the United States, without first obtaining an export license, is a violation of the International Traffic in Arms Regulations. Such violation is subject to a penalty of up to 2 years imprisonment and a fine of $100,000 under 22 U.S.C 2778.

Include this notice with any reproduced portion of this document.

If your address has changed or if you wish to be removed from the RADC mailing list, or if the addressee is no longer employed by your organization, please notify RADC (EEC) Hanscom AFB MA 01731. This will assist us in maintaining a current mailing list.

Do not return this copy. Retain or destroy.

UNCLASSIFIED

SECURITY CLASSIFICATION OF THIS PAGE (When Data Entered)

REPORT DOCUMENTATION PAGE	READ INSTRUCTIONS BEFORE COMPLETING FORM
1. REPORT NUMBER: RADC-TR-80-14	2. GOVT ACCESSION NO.: AD-A088 806	3. RECIPIENT'S CATALOG NUMBER
4. TITLE (and Subtitle): ON THE APPLICATION OF THE GTD-MM TECHNIQUE AND ITS LIMITATIONS	5. TYPE OF REPORT & PERIOD COVERED: Phase Report
	6. PERFORMING ORG. REPORT NUMBER: ESL-711353-1
7. AUTHOR(s): John N. Sahalos, Gary A. Thiele	8. CONTRACT OR GRANT NUMBER(s): F19628-78-C-0198
9. PERFORMING ORGANIZATION NAME AND ADDRESS: The Ohio State University ElectroScience Laboratory, Department of Electrical Engineering, Columbus OH 43212	10. PROGRAM ELEMENT, PROJECT, TASK AREA & WORK UNIT NUMBERS: 2305, 2305J432, 34
11. CONTROLLING OFFICE NAME AND ADDRESS: Deputy for Electronic Technology (RADC/EEC) Hanscom AFB MA 01731	12. REPORT DATE: July 1980
	13. NUMBER OF PAGES: 38
14. MONITORING AGENCY NAME & ADDRESS (if different from Controlling Office): Same	15. SECURITY CLASS. (of this report): UNCLASSIFIED
	15a. DECLASSIFICATION/DOWNGRADING SCHEDULE: N/A

16. DISTRIBUTION STATEMENT (of this Report)

Approved for public release; distribution unlimited.

17. DISTRIBUTION STATEMENT (of the abstract entered in Block 20, if different from Report)

Same

18. SUPPLEMENTARY NOTES

RADC Project Engineer: Ronald G. Newburgh (RADC/EEC)

19. KEY WORDS (Continue on reverse side if necessary and identify by block number)

Geometrical theory of diffraction
Moment method
Wedge diffraction
Scattering
Radar cross section

20. ABSTRACT (Continue on reverse side if necessary and identify by block number)

In 1975 two techniques were published which combined the method of moments and the geometrical theory of diffraction. One technique extended the moment method through the use of the GTD while the second used the moment method to solve for unknown diffraction coefficients thereby extending the use of the GTD. It is the latter method that is considered in this paper and is referred to as the GTD-MM technique.

(Cont'd)

DD FORM 1 JAN 73 1473 EDITION OF 1 NOV 65 IS OBSOLETE

UNCLASSIFIED

SECURITY CLASSIFICATION OF THIS PAGE (When Data Entered)

40 251

Item 20 (Cont'd)

One problem area that existed with the original GTD-MM work was associated with a field incident along or nearly along one wall of a wedge structure. This paper will show an improved series representation for the diffracted current that is sufficient at all incidence angles.

The improved formulation is then applied to the problem of bistatic scattering by a three-sided pyramid. RCS results are obtained which compare very well with experimental measurements. This is believed to be the first use of the GTD-MM technique in treating a 3-dimensional geometry.

SUMMARY

The objective of this task was to improve and extend the usefulness of the GTD-MM technique and to determine the limitations of the method. The GTD-MM technique is a method which combines two applications oriented theories in electromagnetic theory, namely the geometrical theory of diffraction (GTD) and the method of moments (MM). As such, the GTD-MM technique is one of several different methods known as a hybrid technique.

The technical problems addressed in this report are: (1) to overcome certain restrictions in the original GTD-MM work and, (2) to apply the resulting improved formulation to a three-dimensional problem, that of calculating the radar crosssection of a three-sided pyramid. Results were obtained which compared very well with experimental measurements. The results were calculated using a medium sized digital computer and modest amounts of CPU time.

One of the limitations of the GTD-MM technique discussed in the present work is the need for an a priori knowledge of the *form* of the current in the GTD region of the problem. The work in this report suggests that this difficulty may in some cases by overcome by using a suitable series expansion of the current. Future research should examine this approach from a more general viewpoint and should also be directed toward the application of the method to geometries of a three-dimensional nature for which the diffraction coefficient is unknown.

In general, hybrid techniques hold good promise for eventually being able to treat radar scattering problems of quite general and detailed shape. Partly for this reason, a hybrid technique such as the one reported here, is an important research problem.

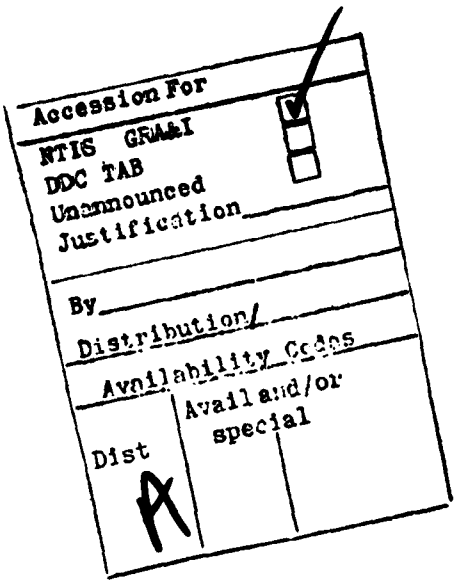

TABLE OF CONTENTS

I. INTRODUCTION

In recent years the geometrical theory of diffraction (GTD), or one of its improved modern versions such as the uniform theory of diffraction (UTD), has become one of the more useful methods for finding solutions to antenna and scattering problems [1]. The applications of diffraction theories are, however, limited to geometries for which the diffraction coefficient is known.

Recently a technique [2] has been developed for extending the use of the GTD by the method of moments (MM) [3]. In this extended GTD-MM technique the diffraction coefficient is treated as an unknown, thereby permitting a larger class of problems to be treated with the GTD. This technique [2] required special consideration for those cases where the incident ray was nearly tangent to one of the faces of the wedge and the results where dependent upon the location of the match points used. In this paper these difficulties are overcome by using a series of three terms based on approximate expressions for the Fresnel integral. Thus, a purpose of this paper is to show that accurate results are obtained with the three term series for all incidence angles, particularly for grazing incidence, and that these results are independent of the location of the match points.

Previously, the (improved) extended GTD-MM technique has been applied to 2-dimensional problems. In this paper we will use the extended GTD-MM technique to treat a 3-dimensional geometry, the three sided pyramid. Thus, a second purpose of this paper is to demonstrate the applicability and limitations of the extended GTD-MM technique to 3-dimensional geometries. As such it represents a first step in applying the extended GTD-MM technique to 3-dimensional problems.

II. INFINITE WEDGE FORMULATION

The infinite wedge is, of course, a canonical (2-dimensional) problem in the GTD and UTD. It is used in this paper merely as a basic geometry to test the methods that follow. That is, the wedge diffraction coefficient is treated as an unknown and solved for numerically. Once the numerical diffraction coefficient is obtained, it may then be compared with the known UTD diffraction coefficient or with the classical (exact) theory solution of the wedge problem [4] to validate the numerical result.

Consider Figure 1 which shows the surface of a wedge divided into

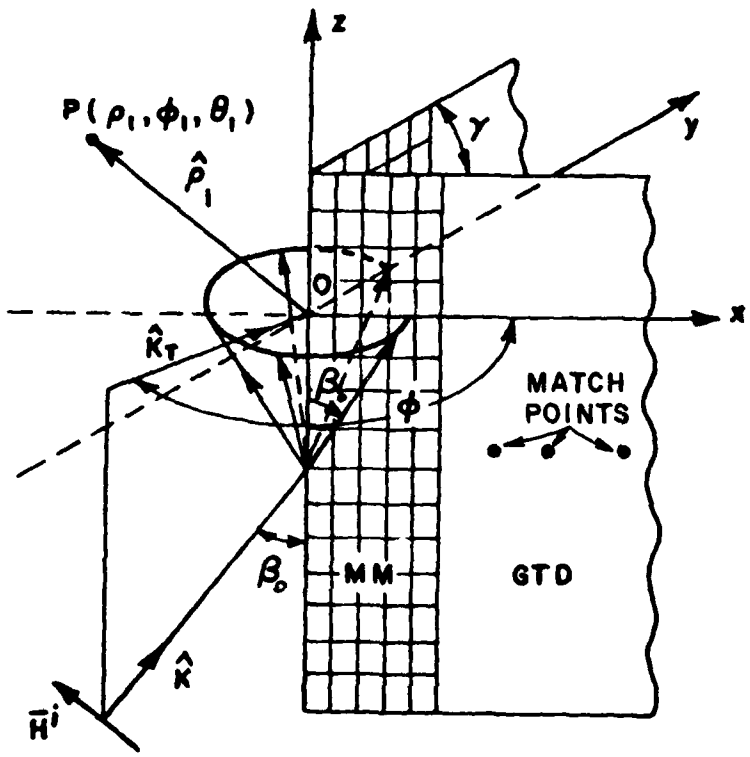

Figure 1. Wedge diffraction geometry used in GTD-MM solution.

two regions. The basic approach here is to use a pulse basis moment method representation for the current near the diffracting edge (i.e.,

MM region), and GTD current forms outside the moment method region. Thus, the current in the GTD region is given by

$$\bar{J}^{GTD} = \bar{J}^{i} + \bar{J}^{r} + \bar{J}^{d} \tag{1}$$

where $\bar{J}^{i}$, $\bar{J}^{r}$ and $\bar{J}^{d}$ are the currents associated with the incident, reflected and diffracted fields respectively.

The currents in the MM region are found using the magnetic field integral equation

$$\bar{J}(\bar{r}) = \hat{n} \times \bar{H}^{i} - \hat{n} \times \iint_{\substack{\text{WEDGE} \\ \text{SURFACE}}} \bar{J}(\bar{r}') \times \nabla G(\rho,\rho')\, ds' \quad . \tag{2}$$

The current may be represented by the components $\bar{J}_T$ in the xy plane and J_z in the xz or yz plane as suggested by Figure 2. Thus,

$$\bar{J}(\bar{r}') = \bar{J}_z(x,y') + \bar{J}_T(x,y') \; . \tag{3}$$

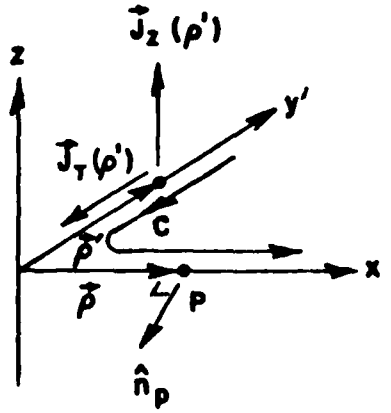

Figure 2. Current of a point ρ' used in magnetic integral equation.

Using Equation (3) in Equation (2) we obtain

$$\bar{J}_T(\rho) = \hat{n}_p \times \bar{H}_z^{i}(\rho) - \hat{n}_p \times \int_C \bar{J}_T(\rho') \times \nabla_T G(\rho,\rho')\, dc' \tag{4}$$

and

$$\bar{J}_z(\rho) = \hat{n}_p \times \bar{H}_T^i - \hat{n}_p \times \int_C \bar{J}_z \times \nabla_T G(\rho,\rho')\, ds'$$

$$- j k_z \hat{n}_p \times \int_C \bar{J}_T G(\rho,\rho')\, dc' \qquad (5)$$

where $G(\rho,\rho')$ is the two-dimensional Green's function written in terms of the Hankel function $H_o^{(2)}$ as

$$G(\rho,\rho') = \frac{1}{4j} H_o^{(2)}(k_T|\bar{\rho}-\bar{\rho}'|), \qquad (6)$$

where $k_T = k \sin\beta_o$. The del operator is given by

$$\nabla = \nabla_T + \nabla_z = \nabla_T + \hat{z}\frac{\partial}{\partial z} \qquad (7)$$

and the currents are related to the magnetic field by

$$\bar{J}_z = \hat{n}_p \times \bar{H}_T \qquad (8)$$

and

$$\bar{J}_T = \hat{n}_p \times \bar{H}_z \quad . \qquad (9)$$

In the extended GTD-MM technique it is necessary to assume the <u>form</u> of the diffracted current $\bar{J}^d$ in Equation (1). In Reference 2, Burnside, et. al. took the diffracted current to be proportional to $e^{-jk\rho}/\sqrt{\rho}$. This is satisfactory except when the shadow boundary of the incident field is near one wall of the wedge as the authors point out. In this special case they proposed the series

$$J^d = \sum_{n=0}^{\infty} D^{(n)} \frac{e^{-jk\rho}}{(\sqrt{\rho})^n} \qquad (10)$$

and found that the first two terms gave good results but that the solution was "somewhat dependent on the locations of the sample (match) points". The reason they [2] had this sensitivity to match point location was that the series in Equation (10) does not adequately represent the current in the case of grazing incidence. That is to say, an a priori knowledge of the form of the current was not available in this instance.

To overcome the difficulties mentioned above, let us examine the wedge diffraction coefficient in its Fresnel integral form. (We do this merely to gain sime insight into what the form of the current really should be. We will not use any of the well-known diffraction coefficient expressions in the numerical calculations which follow later.) Consider the wedge in Figure 3a. If the incident ray is in region I, then there are two reflected rays R_0 and R_1 as shown. The diffracted current in the x wall can be viewed as being generated by three rays as shown in Figure 3b. Thus the diffracted current on each wall will be the summation of the three currents associated with the three rays where incidence angles are listed below

	xz plane	yz plane
1.	ϕ	$360 - \phi - \gamma$
2.	$360 - \phi$	$\phi - \gamma$
3.	$360 - \phi - 2\gamma$	$\phi + \gamma$

We know that each of the three diffracted currents may be written in Fresnel integral form. Thus, for the wall in the xz plane we have:

$$J_{1x}^{d} = D_x(\phi)\, e^{+jk_T\rho\cos\phi} \int_{\sqrt{k_T\rho(1-\cos\phi)}}^{\infty} e^{-j\tau^2} d\tau \qquad (11)$$

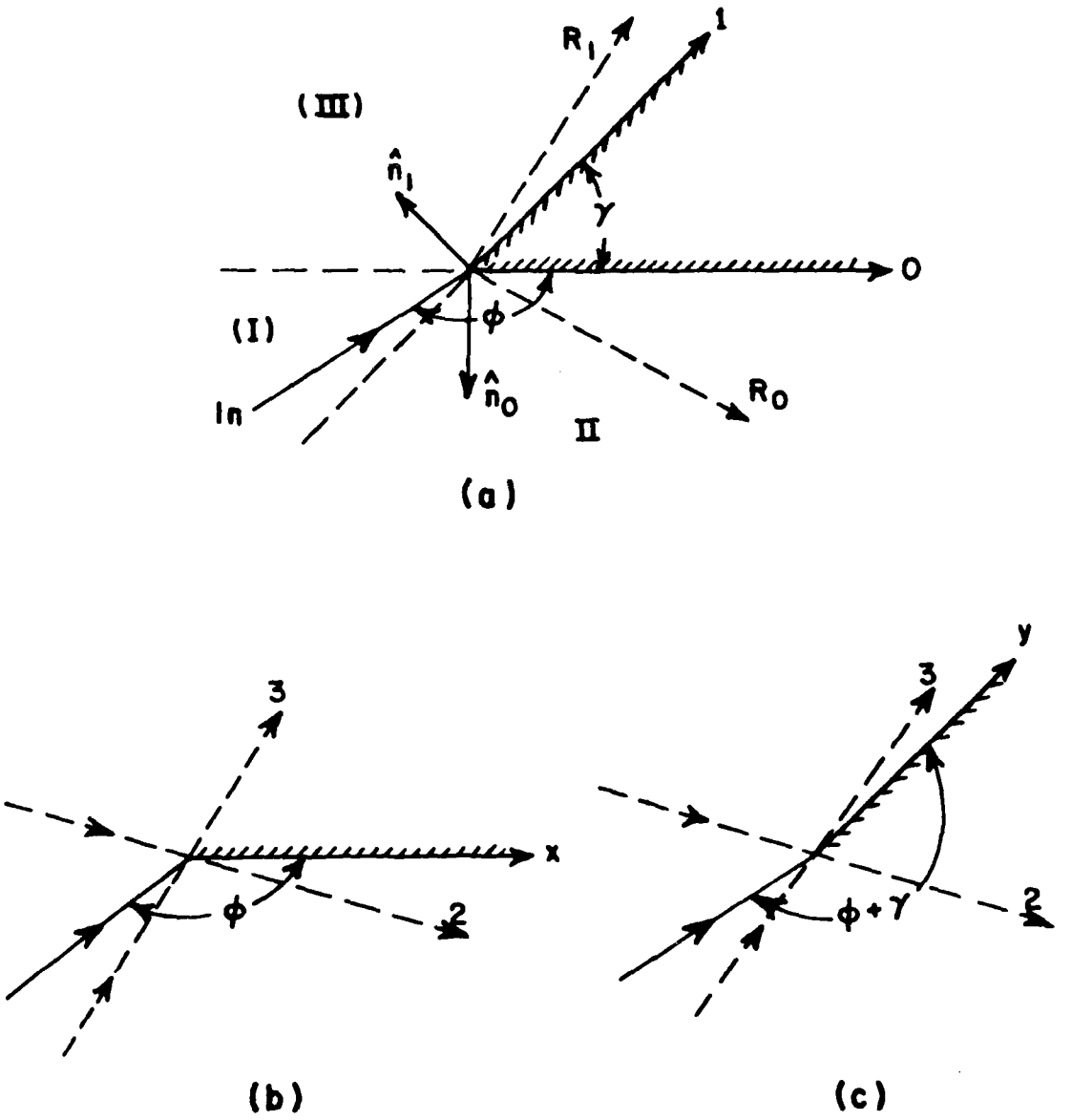

Figure 3. Wedge reflection geometry.

$$J_{2x}^{d} = D_x(360-\phi)\, e^{+jk_T\rho\cos\phi} \int_{\sqrt{k_T\rho(1-\cos\phi)}}^{\infty} e^{-j\tau^2} d\tau \qquad (12)$$

$$J_{3x}^{d} = D_x(360-\phi-2\gamma)\, e^{+jk_T\rho\cos(\phi+2\gamma)} \int_{\sqrt{k_T\rho(1+\cos(\phi+2\gamma))}}^{\infty} e^{-j\tau^2} d\tau \,. \qquad (13)$$

Similar expressions can be written for the other wall of the wedge.

From [5] it can be shown that a Fresnel integral may be approximated as follows:

$$\int_{\sqrt{\alpha}}^{\infty} e^{-j\tau^2} d\tau \simeq \sqrt{\frac{2}{\pi}}\,(a_0 + a_1\sqrt{\alpha}), \qquad \text{if } \sqrt{\alpha} \to 0 \qquad (14)$$

and

$$\int_{\sqrt{\alpha}}^{\infty} e^{-j\tau^2} d\tau \simeq \sqrt{\frac{2}{\pi}}\,\frac{a_2}{\sqrt{\alpha}}, \qquad \text{if } \sqrt{\alpha} >> 1 \qquad (15)$$

where a_0, a_1 and a_2 are coefficients independent of α which may be evaluated from [5].

If none of the 3 rays is near the x axis, then Equation (15) applies and we have

$$J_x^{d} = J_{1x}^{d} + J_{2x}^{d} + J_{3x}^{d} \simeq D_x \frac{e^{-jkx}}{\sqrt{x}} \qquad (16)$$

as we would expect. On the other hand, if any one of the three rays is near the x-axis, then either $\frac{2}{\pi} k_T x(1+\cos\phi) << 1$ due to ϕ being close to 180^0, or $\frac{2}{\pi} k_T x(1+\cos(\phi+2\gamma)) << 1$ due to $(\phi+2\gamma)$ being close to 180^0. In this case, since some of the rays are near grazing and some are not, both Equations (14) and (15) apply and we must write

$$J_x^d = J_{1x}^d + J_{2x}^d + J_{3x}^d = D_x^{(-1)} \frac{e^{-jk_T x}}{\sqrt{x}} +$$

$$+ D_x^{(o)} e^{-jk_T x} + D_x^{(1)} e^{-jk_T x} \sqrt{x} \quad . \qquad (17)$$

The superscript on the diffraction coefficients is associated with the value of n for $\frac{1}{(\sqrt{x})^{-n}}$.

We could reach the same conclusion given by Equation (17) by examining the Kouyoumjian-Pathak diffraction coefficient [1] or the spectral Theory of Diffraction work of Mittra, et al. [6]. For example, in the former, for $\phi=0$, $a^+(-\phi')=a^-(\phi')=1+\cos\phi'$ and the four terms in the diffraction coefficient reduce to three. Each of those three terms may be identified with one of the terms in Equation (17).

Equation (17) is valid for all values of x except near the source of diffraction where the form of the current is not known. Therefore Equation (17) applies when x > minimum value of either ρ_1^x or ρ_2^x where, from the conditions discussed between Equations (16) and (17), we obtain

$$\rho_1^x = \frac{\lambda}{4(1+\cos\phi)} \qquad (18)$$

and

$$\rho_2^x = \frac{\lambda}{4[1+\cos(\phi+2\gamma)]} \quad . \qquad (19)$$

Thus, the approximation of the total current on the x-axis will be

$$J_x = \begin{cases} \sum_{m=1}^{N} a_m^x P(x-x_m) \quad , & 0<x<\min(\rho_1^x, \rho_2^x) \\ J_x^i + J_x^r + \sum_{n=-1}^{1} D_x^{(n)} \frac{e^{-jk_T x}}{(\sqrt{x})^{-n}} \quad , & \min(\rho_1^x, \rho_2^x)<x<\infty \end{cases} \qquad (20)$$

where $P(x-x_m)$ is a pulse function with complex coefficient a_m.

The same procedure can be used to write an expression for the current on the other face of the wedge. Then, following the same procedure as given in [2] we can solve for the unknown pulse weights a_m and the unknown diffraction coefficients $D_x^{(n)}$ and $D_y^{(n)}$, except that there will be 3 match points on each face of the wedge in the GTD region instead of only one or two as in [2]. Therefore the system of equations to be solved will be at most of order 2N+6 where N will typically be a small number (i.e., 2 or 3 or 4).

III. INFINITE WEDGE RESULTS

Results have been run for a variety of incidence angles from grazing to normal incidence and for wedges with a variety of interior wedge angles. In all cases the three term series in Equation (17) yields results which are in excellent agreement with the exact classical theory [4]. We will discuss one typical case here. Consider Figure 4 which shows a plane wave incident on a 30^0 wedge with the electric field perpendicular to the edge of the wedge. Two results are shown, one when the wave is 5^0 from grazing upon the y' wall and the other when the wave is 5^0 from grazing upon the x wall. Both results are in perfect agreement with the exact theory.

The results in Figure 4 could have been generated by using fewer than 6 unknowns in the two GTD regions. That is, in the $\phi=155^0$ case where no rays are close to tangency with the x wall, the $D_x^{(0)}$ and $D_x^{(1)}$ terms could be omitted. Indeed the computer print out shows them to be relatively unexcited. Similarly, for the $\phi=175^0$ case the $D_y^{(0)}$ and $D_y^{(-1)}$ terms could be omitted since no rays are close to tangency with the y' wall. Conversely, if any of the essential terms are omitted, incorrect results will be obtained for the currents on the faces of the wedge for those cases where there are rays close to tangency with one of the faces of the wedge [7]. This fact is well-illustrated by the results in Figures 5 and 6. In Figure 5 a ray is exactly grazing

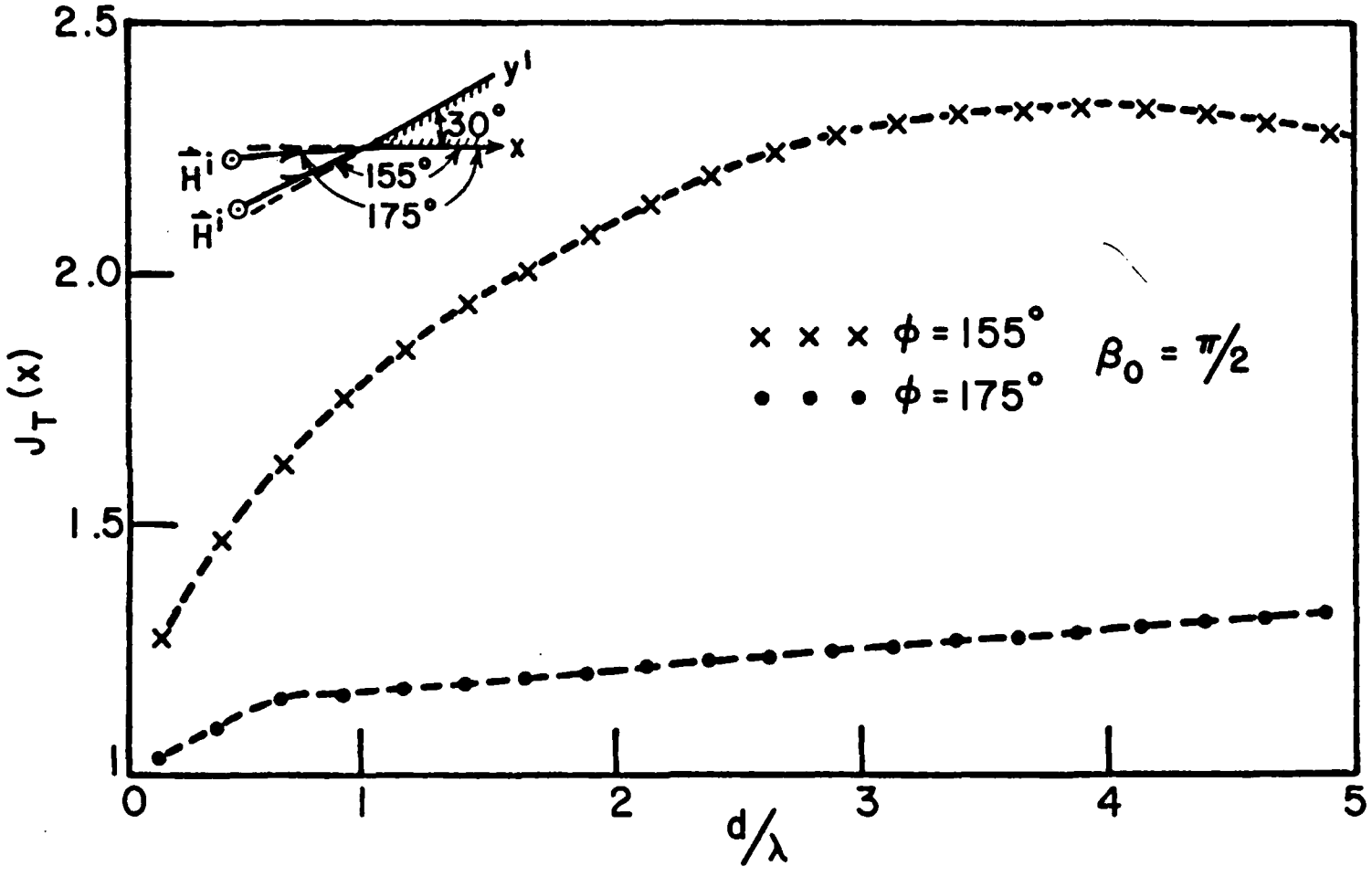

Figure 4a. Magnitude of the currents along x-wall of 30^0 wedge for two normal incidence cases near the shadow boundaries.

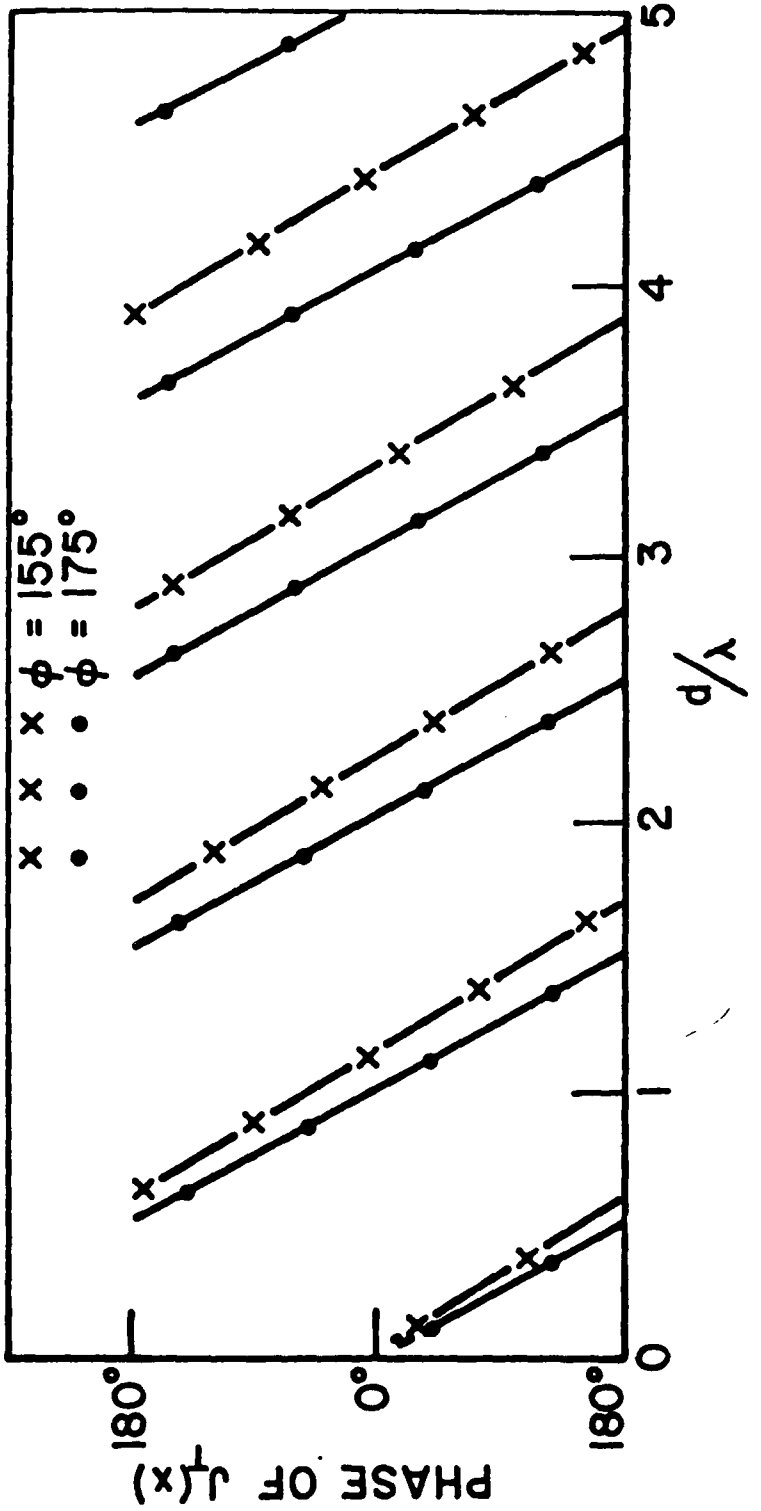

Figure 4b. Phase of the current along x-wall of 30^0 wedge for two normal incidence cases near the shadow boundaries.

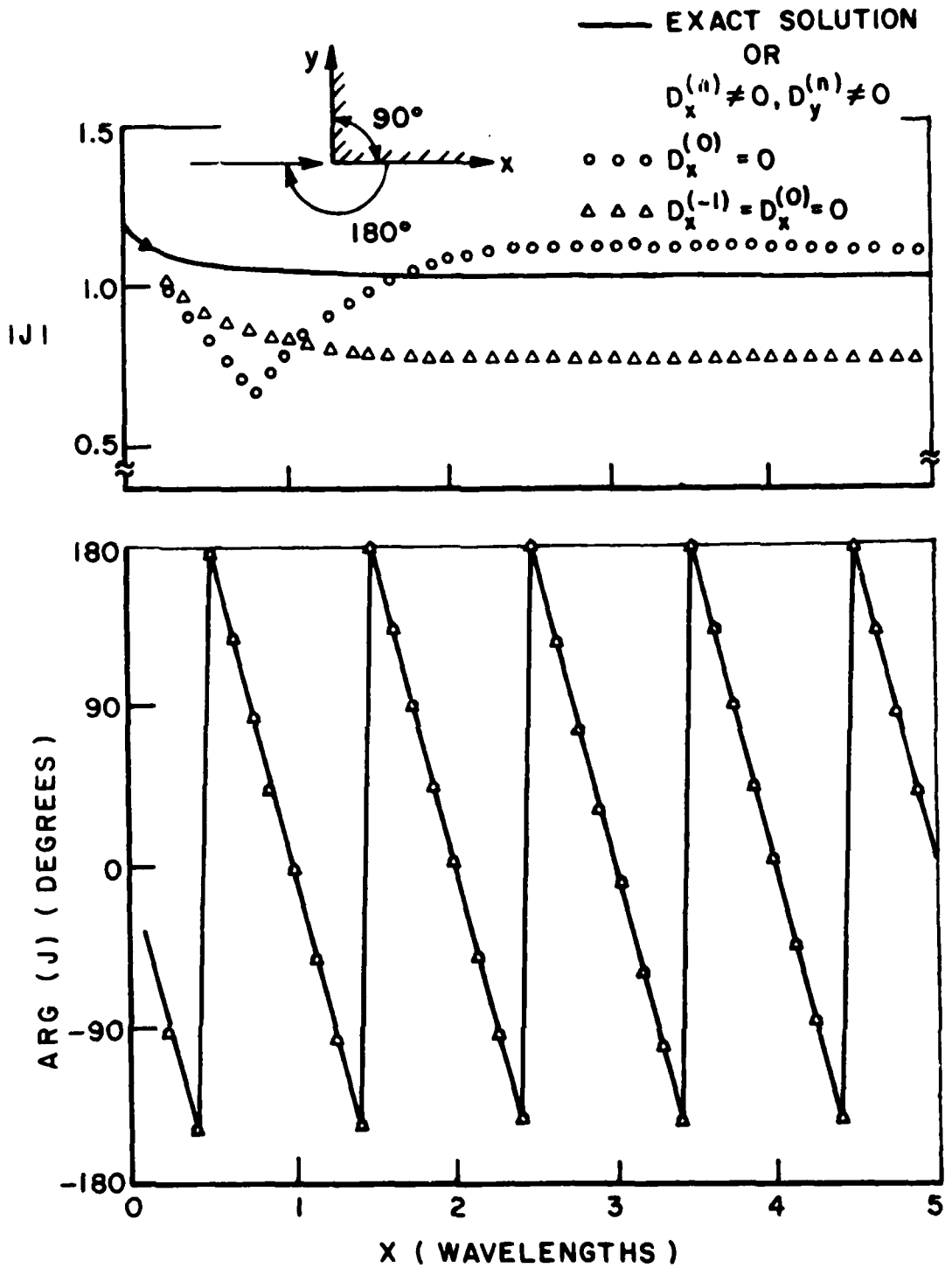

Figure 5. Current along x-wall for various combinations of coefficients compared to exact solution.

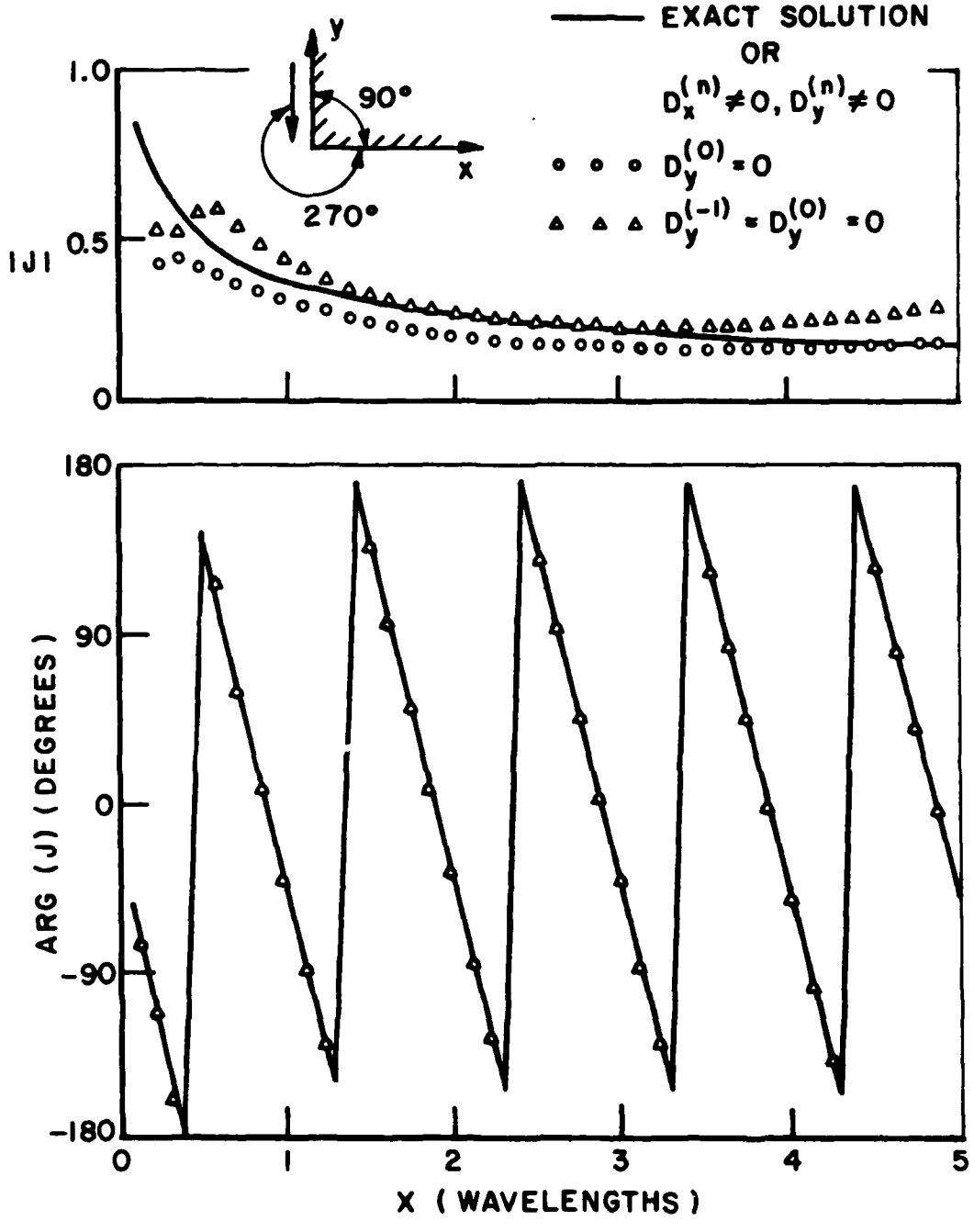

Figure 6. Current along y-wall for various combination of coefficients compared to exact solution.

upon the x wall of a wedge. Exact agreement is obtained when all terms are used. However, if one or both of $D_x^{(0)}$ and $D_x^{(-1)}$ are zero, the incorrect current magnitude is obtained although the phase is unaffected. Figure 6 shows a ray exactly grazing upon the y wall in the "opposite" direction. Similar observations to those made for Figure 5 can be made. for Figure 6.

For the results generated above, typically the three match points were located between a distance of 1λ and 5λ from the wedge edge for a grazing incidence case and between 0.5λ and 5λ for non-grazing incidence cases. An objection has been raised [8] that in the grazing incidence cases, the current would grow without limit due to the $D_x^{(1)}$ term. Further investigation beyond [7] showed that this does not occur out to and somewhat beyond the location of the most distant match point, even when it is located several hundred wavelengths from the wedge edge. Such a large distance is adequate for most problems of interest and much more than adequate for the pyramid problem in the next section. It should be noted that a slow rise in the current in a grazing incidence case (e.g. Figure 4, $\phi=175^o$ case) is natural since the wave will continually reinforce the current along the wall until some saturation point is reached. Indeed it is the $D^{(1)}$ term that permits this physical phenomena to occur in the calculations even though the numerical value of $D_x^{(1)}$ is always very small.

Figure 7 illustrates the behavior of the three coefficients with incidence angle for a 30^o wedge. Note that $D_x^{(1)}$ is always the smallest coefficient except when $\phi\approx 180^o$, the grazing incidence case. In this case the $D_x^{(0)}$ coefficient dominates as expected. Note too that when ϕ is not near 180^o, the $D_x^{(-1)}$ coefficient dominates as one would expect, and that the $D_x^{(1)}$ coefficient is from two to four orders of magnitude lower.

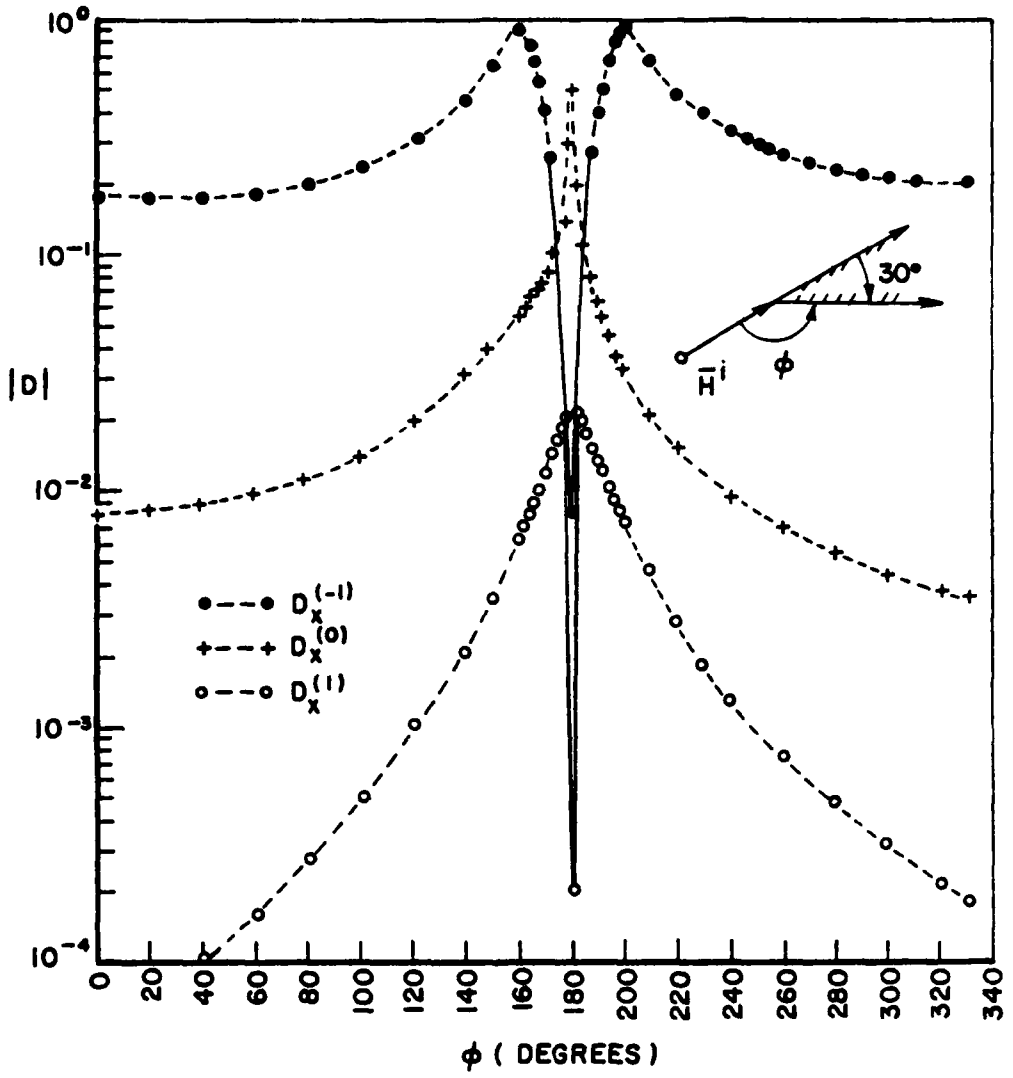

Figure 7a. Variation of the numerical coefficient magnitude with incidence angle.

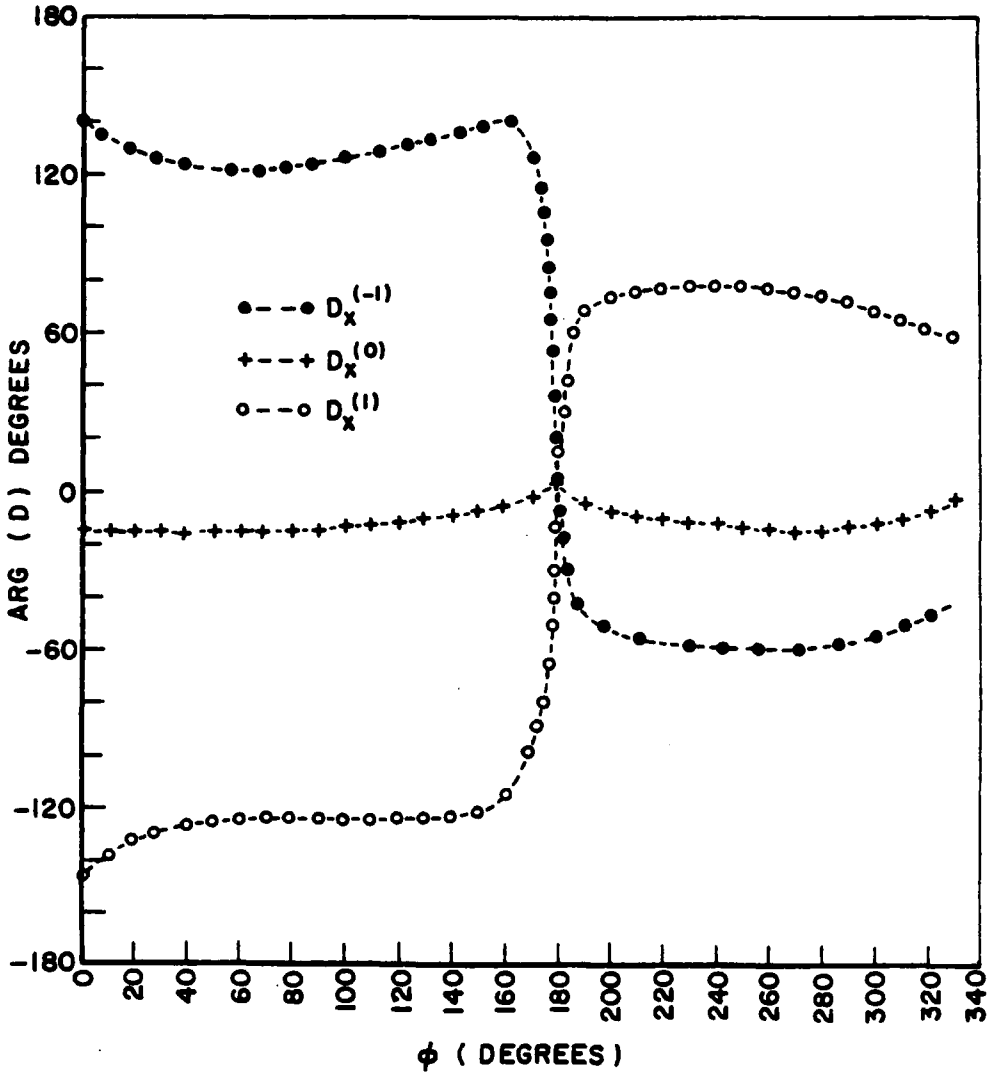

Figure 7b. Variation of the numerical coefficient phase with incidence angle.

In this paper, the extent of the MM region is $\lambda/2$. A larger size (e.g., 1λ) can be used if the number of expansion functions is proportionately increased.

And finally, we should remark that although the results in this section show the three term series in Equation (17) to be sufficient in all cases, one could possibly conceive of a series with more terms. However, such a series may be divergent as is sometimes the case with such asymptotic solutions.

The results in this section show that the three term series in Equation (17) is certainly a correct one to use. In this problem we were fortunate in having considerable knowledge about the known asymptotic solution for the problem which we could look at to deduce the correct series expression for the current. However, in the general useage of the GTD-MM technique this would probably not be true which is one of the points of this paper.

IV. THREE-SIDED PYRAMID FORMULATION

For the problem of scattering by a pyramid (i.e. a 3-dimensional problem) as treated in this paper, each face of the four faces of the 3-sided pyramid (i.e. three sides plus base) is composed of two regions, a GTD region and a MM region along each of the three edges of any one face as illustrated by Figure 5. The current distribution on the surfaces is found by solving the 2-dimensional wedge diffraction problem once for each wedge or a total of six times for the entire problem. Thus the current in the GTD region is the superposition of the diffracted currents from the three 2-dimensional solutions applicable to a particular face plus the currents due to the incident and reflected fields. For example, the current in Figure 6 at point M in a GTD region is the summation of the five currents J_1^d, J_2^d, J_4^d, J^i and J^r. The first three currents are due to diffraction from edges 1, 2 and 4 respectively while

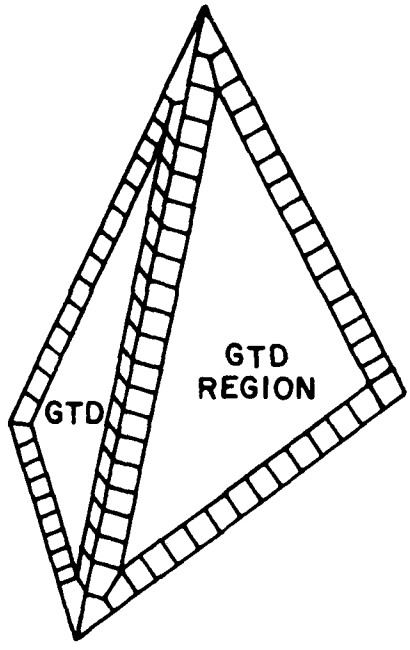

Figure 8. Pyramid faces with GTD and MM regions.

J^i and J^r are due to the incident and reflected fields as discussed in Section II.

The current along the edges of each face is obtained from the corresponding 2-dimensional wedge diffraction solution (MM part) plus the diffracted currents from the other 2 edges plus, of course, the currents associated with the incident and reflected fields.

To obtain the scattered field we use the radiation integral for the current in the MM region as well as for the current in the GTD region. This is necessary because in the method used here, we can define the "numerical diffraction coefficients" only on the faces of the object (i.e., pyramid) and not as a function of the angle of the observation point. Thus, it is necessary to use the current rather than use ray tracing as is done in the usual use of the GTD.

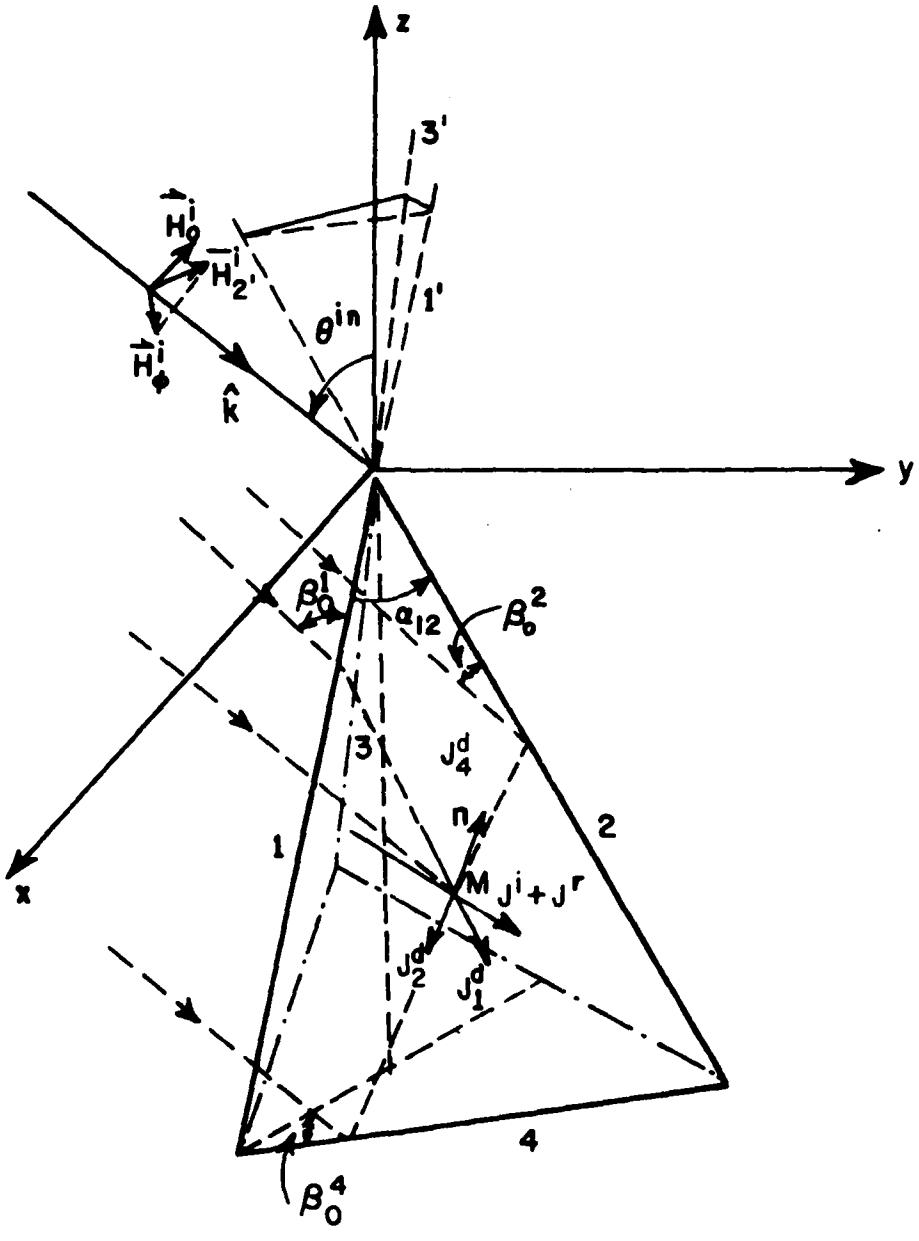

Figure 9. Geometry for one face of the triangular pyramid.

The solution for the current obtained in the manner described above constitutes a first step in the solution process that is probably sufficient for most backscatter problems. A refinement (i.e. a second step) will be discussed later. Note that the solution neglects multiple diffractions from the edges and also neglects diffractions from the three vertices on any given face. We will refer to the latter as tip diffraction.

For bistatic scattering the effect of tip diffraction may be added post facto to the scattered field obtained by integrating over the surfaces of the pyramid visible in the desired direction of the scattered field. The tip diffracted field may be evaluated by using a tip diffraction coefficient given by Keller, et al [9] which is also discussed in [8]. The tip diffraction coefficient formula is for a plane corner with two straight edges meeting at an angle and is of the form

$$C_{\perp} = \frac{j}{4\,k_o} \frac{(\cos\theta+\cos\theta')\sin\delta}{(\cos a-\cos a')(\cos b-\cos b')} \qquad (21)$$

where a and b are the angles between the incident field and the two edges at the corner; a' and b' are the angles between the diffracted field at the two edges; θ and θ' are the angles between the normal to the plane of the corner and the incident and diffracted rays; and δ is the angle between the two edges. The perpendicular symbol in $C_{\perp}$ denotes that only that transverse component of the incident electric field which is not parallel to the plane of the corner is used to determine the tip diffracted field. The fact that the vertices in this problem do not constitute plane corners is ignored in applying Equation (21) since it may be argued that the non-plane nature of the vertices is a negligible deviation for the tips on the pyramid. It will be seen in the next section that inclusion of the tip diffracted field does noticeably and favorably raise the level of the radar cross section results at most aspect angles but the scattering "pattern" is little changed by the tip diffracted field.

Unfortunately there is at present no satisfactory vector electromagnetic diffraction coefficient available for corner diffraction. We used Keller's formula for the transverse component of the incident electric field without first investigating the limitations of the formula itself, if in fact there are any. Keller's formula gave quite good results over a wide range of aspect angles. There is another formula in 11 in Figures 118-120 due to the work of Felsen. This tip diffraction formula is for cones and is restricted to small incidence angles with respect to the axis of the cone.

The tip diffraction contribution may be included in a different or alternative manner. Using the tip diffraction coefficient in Equation (21) one can obtain a tip diffracted current contribution to the current in the GTD region. Thus, at point M in Figure 9 there could also be shown three tip diffracted rays giving rise to currents J^d_{t12}, J^d_{t24} and J^d_{t14} where, for example, J^d_{t12} is the diffracted current from the tip formed by edges 1 and 2. Next,one considers the current on the surface in the immediate vicinity of each of the twelve tips to be unknown. Using the now known current on each face (i.e. both in the MM and GTD regions), one can generate an incident field at each of the twelve tip regions and employ Equation (2) to solve for the current at and near each tip. This is the second step in solution mentioned earlier in this section but not discussed in [12]. If this step is carried out accurately, the same scattered field will be obtained as when the tip diffracted field is added on post facto. However, including the tip diffraction contribution in the current permits a more accurate representation of the current than that obtained in the first step. The second step described here is used in the next section to obtain the plots of the current distribution.

V. THREE-SIDED PYRAMID RESULTS

In the results which follow for the 3-dimensional pyramid problem, the edges numbered 1, 2, and 3 in Figure 9 are all of length 9.144λ and make an angle of 15^{0} with the z-axis.

Using the second step discussed in the previous section, the magnitude of the current distribution was obtained for the case where a plane wave was normally incident upon edge 4 (see Figure 9) with the magnetic field parallel to this edge. The current distributions are shown on the three faces in Figures 10 and 11 and on the base in Figure 12. Although there was no reasonable way to verify the degree of accuracy of the current distributions, they appear reasonable, have the anticipated behavior in the tip regions, and do produce radar cross section results that agree well with experimental measurements.

The number of pulse expression functions used in the MM region was N=5. The current discontinuity at the boundary between the MM and GTD regions is quite small, too small to be shown in the figures.

Figures 13 and 14 show bistatic radar cross section results when the pyramid is rotated about the z-axis with the incident wave parallel to the xy plane. Figure 13 is for the case where the E-field is parallel to the xy plane (horizontal polarization) and Figure 14 is for the case where the E-field is parallel to the z-axis (vertical polarization). Results are shown both with and without tip diffraction. It is apparent that the inclusion of tip diffraction improves the results at most aspect angles and in fact does bring the results into very close agreement with measurements made in the Ohio State University anechoic chamber. The agreement between the calculations and measurements tends to validate at least the gross accuracy with which the current distribution has been obtained. Further RCS results may be found in [12]. Clearly we could have obtained these RCS results solely using the UTD and Equation

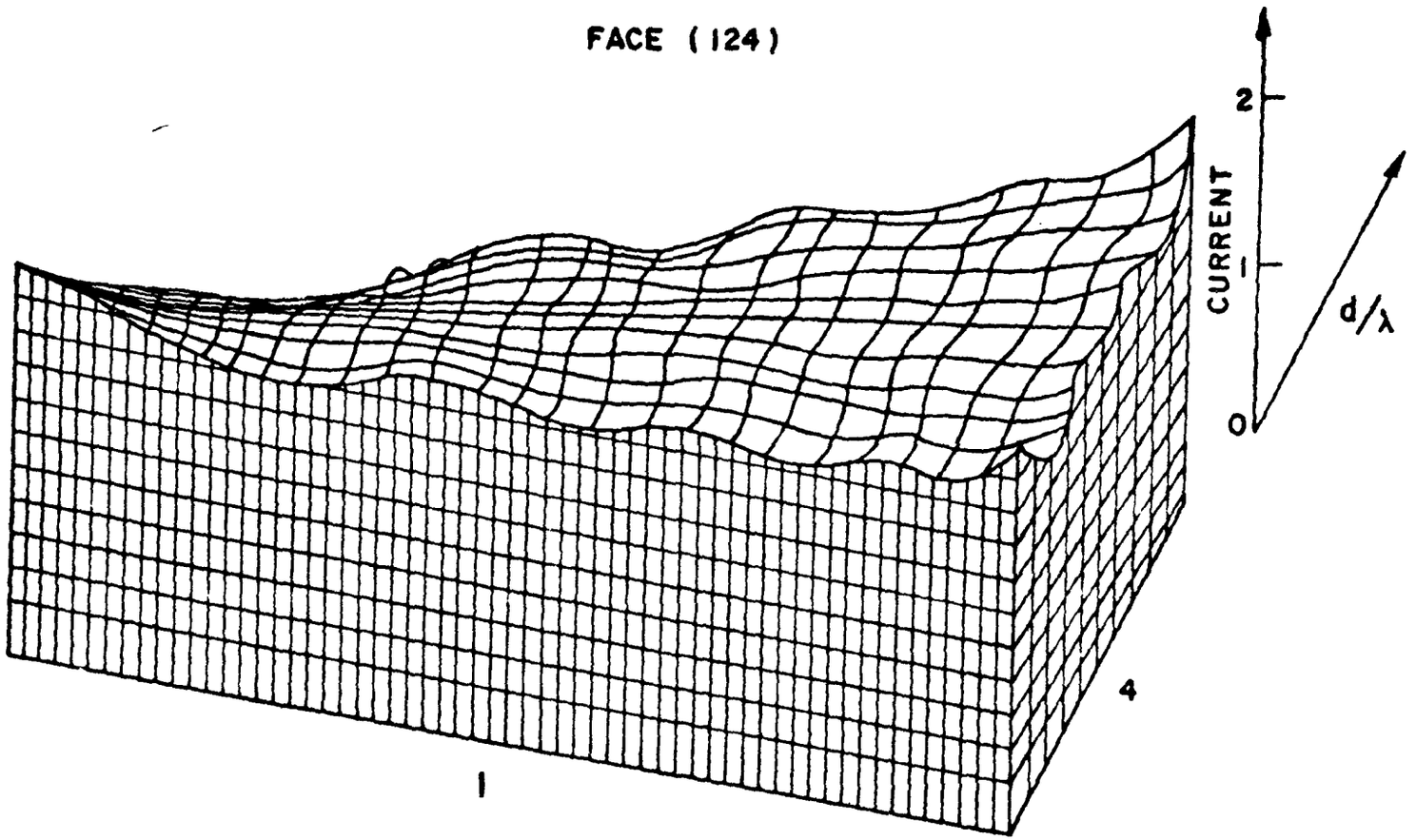

Figure 10. Magnitude of the surface current on face 124 of the pyramid.

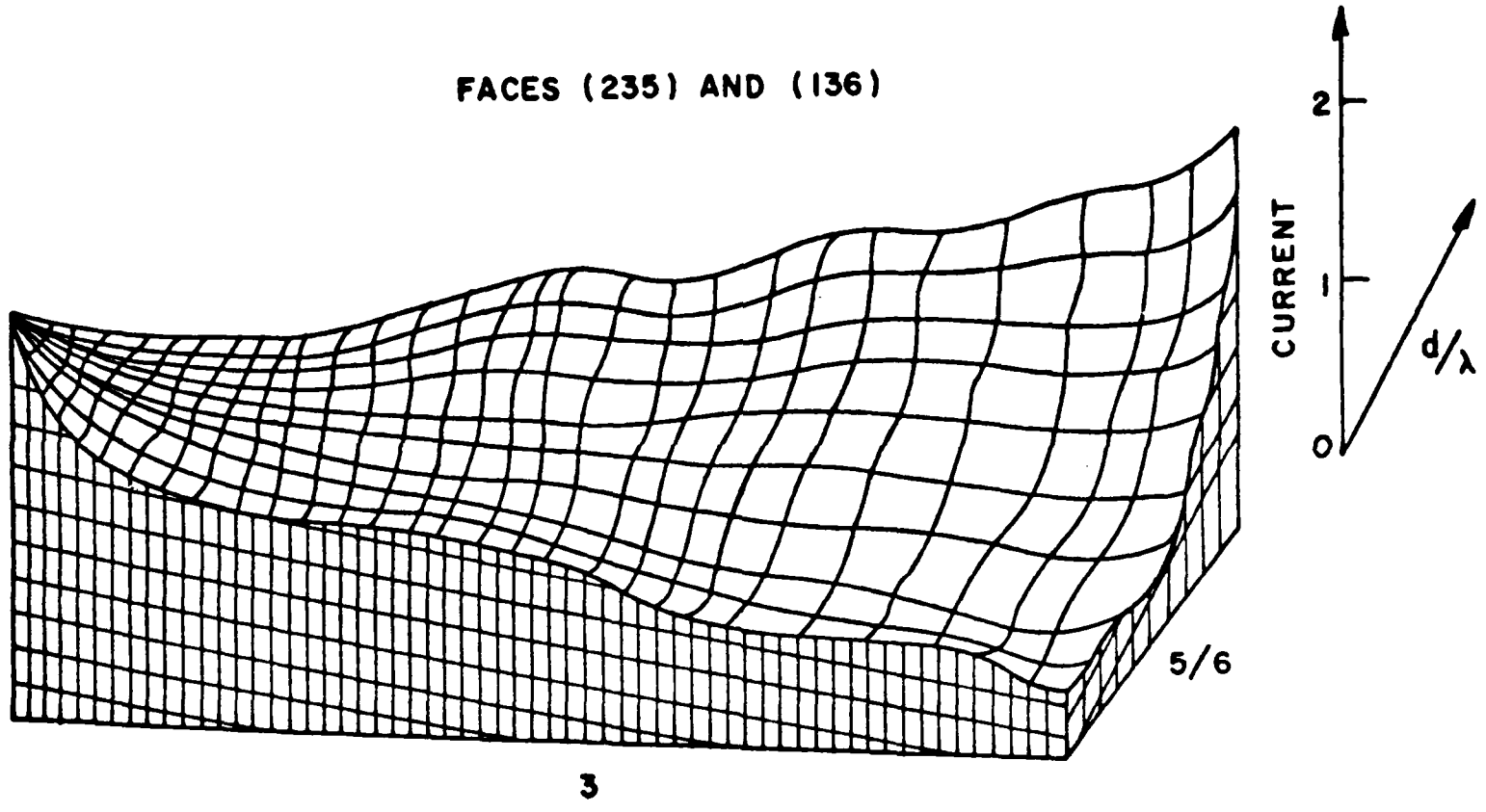

Figure 11. Magnitude of the surface current on either face 235 or 136.

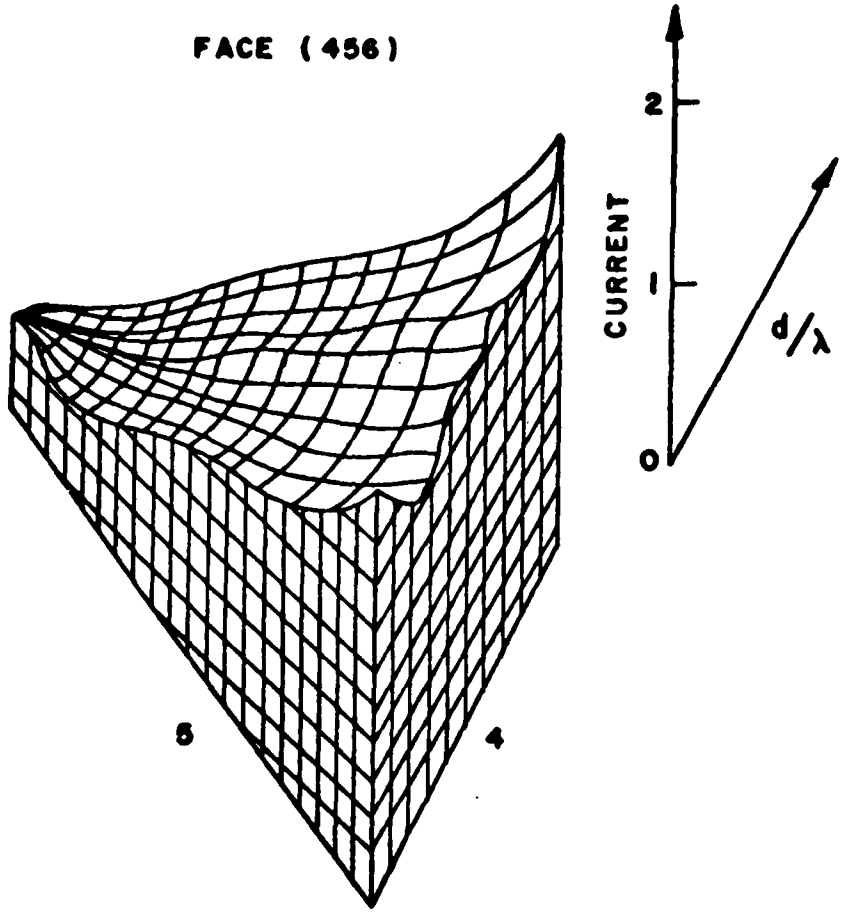

Figure 12. Magnitude of the surface current on face 456, the pyramid base.

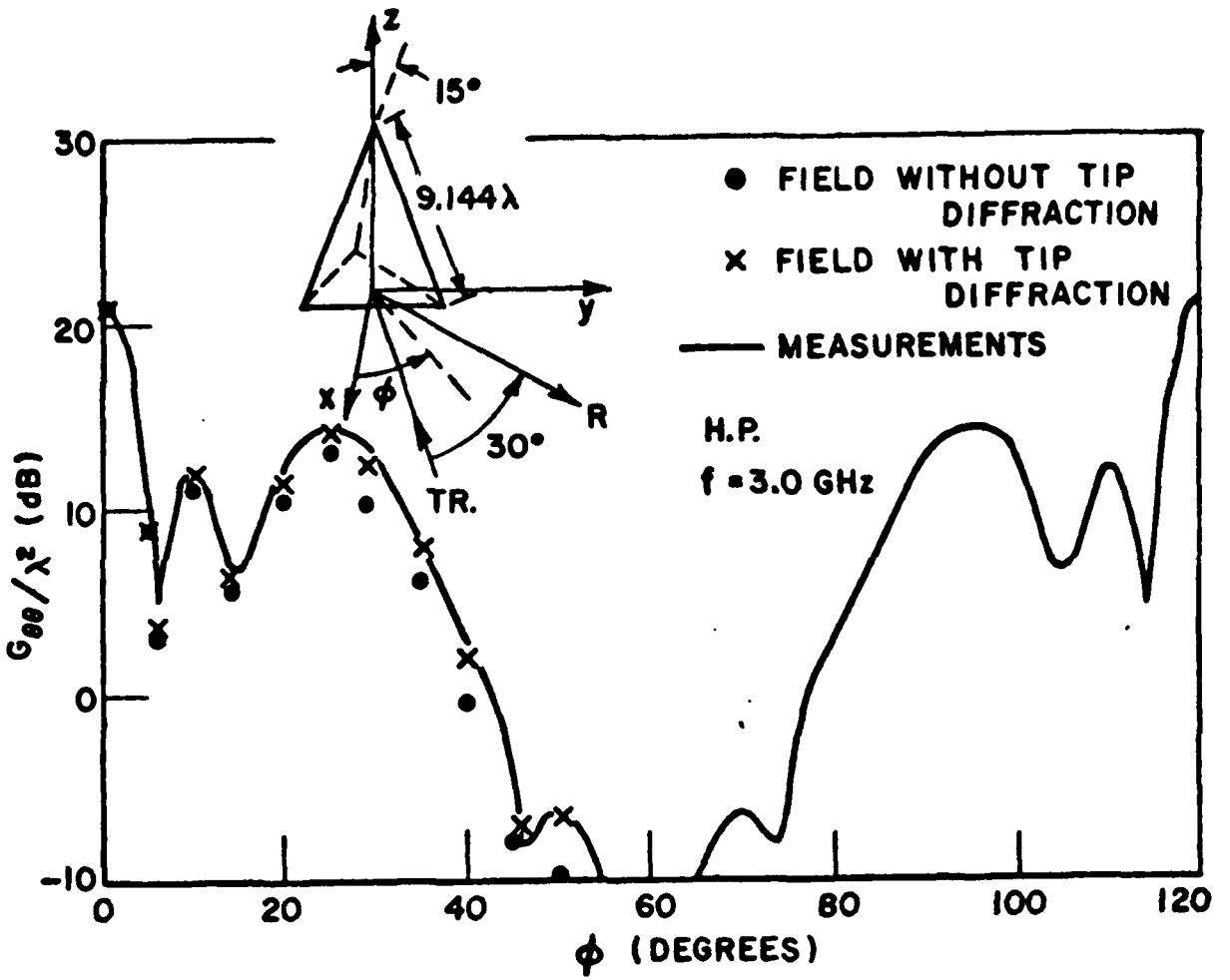

Figure 13. Bistatic (30^{0}) radar cross section for horizontal (ϕ) polarization.

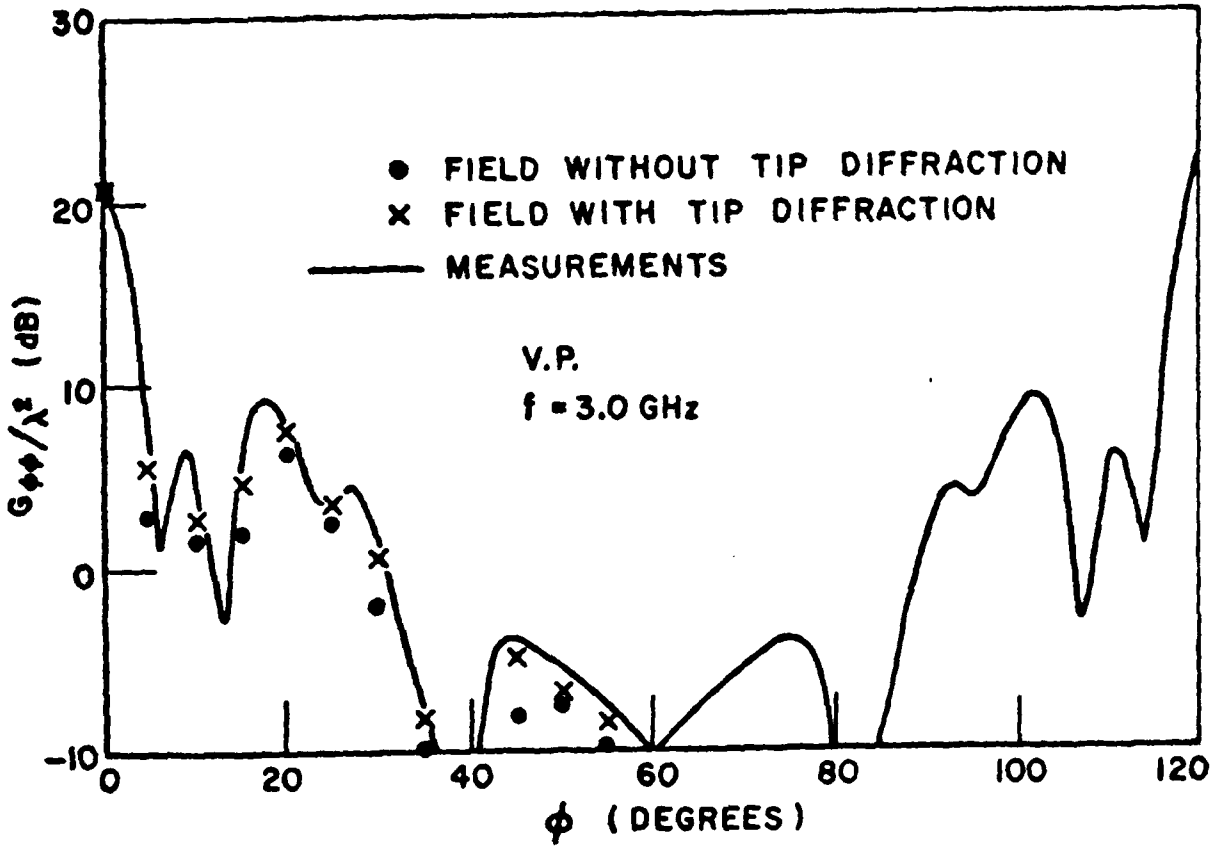

Figure 14. Bistatic (30^{o}) radar cross section for vertical (z) polarization.

(21) but our purpose here has been to apply the extended GTD-MM technique to a 3-dimensional problem.

VI. SOME OBSERVATIONS

The GTD-MM technique permits one to solve for "unknown" diffraction coefficients if one knows the form of the current in the GTD region. In Section II we saw for the wedge that the obvious assumption that the current in the GTD region varies as $(\rho)^{-1/2}$ is invalid in the grazing incidence case. The assumption was corrected to include two other terms which were suggested by the mathematics associated with the known Fresnel integral form of the diffraction coefficient. In retrospect we might have been able to suggest those two additional terms from the physics of the problem. In any case the work in Section II does illustrate the need for good a priori knowledge of the form of the current in the GTD region if the unknown diffraction coefficient is to be correctly determined. In the future treatment of geometries for which the diffraction coefficient is truly unknown, the need for a priori knowledge of the form of the current in the GTD region may prove to be a limitation on the use of the method in certain cases. In fact current work on the vertex diffraction problem indicates the often stated assumption that the current varies as $(r)^{-1}$ is incorrect near the vertex. Nevertheless, the GTD-MM technique does offer a useful procedure for numerically obtaining diffraction coefficients whose analytical form is unknown.

The application of the GTD-MM technique in Section IV to a 3-dimensional problem was based, for the most part, on a superposition of 2-dimensional sub-problems. It would not have been feasible to have solved for all the MM currents on the pyramid simultaneously due to the large matrix that would have resulted. Thus, a superposition of 2-dimensional sub-problems was essential. It may be noted that in [2], Burnside, et al solved the problem of a cylinder with square cross section by solving for the MM currents along all four edges simultaneously.

However, that problem was 2-dimensional. If we wished to solve the finite length cylinder of square cross section (i.e. a 3-dimensional problem) using the GTD-MM technique, it would be necessary to proceed in a manner essentially identical to that used for the pyramid in this paper.

Other problems might be considered by the techniques of Section II and IV. For example, if the three sides of the pyramid were coated with a dielectric material and, perhaps, the base was not, we could 1) solve the 2-dimensional problem of a wedge coated on either one or both sides of the wedge with a dielectric using the GTD-MM technique and 2) solve the coated or partially coated tip problem using the GTD-MM technique, and then 3) superimpose these various 2-dimensional problems to investigate the 3-dimensional coated pyramid problem. It is expected that future developments in the GTD-MM technique will permit such complex geometries to be treated.

REFERENCES

1. R.G. Kouyoumjian, "The Geometrical Theory of Diffraction and Its Application," Chapter 6 in Numerical Asymptotic Techniques in Electromagnetics, R. Mittra, Ed., Springer-Verlag, Berlin, 1975.

2. W. D. Burnside, C. L. Yu and R. J. Marhefka, "A Technique to Combine the Geometrical Theory of Diffraction and the Moment Method," IEEE Transactions on Antennas and Propagation, Vol. AP-23, pp. 551-558, July 1975.

3. R.F. Harrington, Field Computation by Moment Methods, New York, MacMillan, 1968.

4. R.F. Harrington, Time Harmonic Electromagnetic Fields, McGraw Hill, New York, p. 239, 1961.

5. M. Abramowitz and I. Stegum, Handbook of Mathematical Functions, NBS Applied Mathematics Series No. 55, June 1964.

6. R. Mittra, Y. Rahmot-Samii and W. L. Ko, "Spectral Theory of Diffraction," Applied Physics, Vol. 10, pp. 1-13, 1976.

7. J. Sahalos and G.A. Thiele, "An Improved Formulation for Extending The Geometrical Theory of Diffraction by the Moment Method," Report 4372-2, May 1977, The Ohio State University ElectroScience Laboratory, Department of Electrical Engineering; prepared under Contract N00014-76-C-0573 for Office of Naval Research.

8. J. Sahalos and G.A. Thiele, "An Improved Formulation for Extending the GTD Using the Moment Method," presented at the International Symposium on Antennas and Propagation, Sendai, Japan, 29-31 August 1978.

9. J.B. Keller, R.M. Lewis and B.D. Secklar, "Diffraction by an Aperture (II)," J. Appl. Phys., Vol. 28, p. 570, 1957.

10. G.T. Ruck, ed., Radar Cross Section Handbook, Plenum Press, New York, 1970, Vol. 1, p. 48.

11. G. T. Ruck, ed., Radar Cross Section Handbook, Plenum Press, New York, 1970, Vol. 1, pp. 118-120.

12. J. Sahalos and G.A. Thiele, "Bistatic Scattering by a Triangular Pyramid," Report 4372-4, June 1977, The Ohio State University ElectroScience Laboratory, Department of Electrical Engineering; prepared under Contract N00014-76-C-0573 for Office of Naval Research.

MISSION
of
Rome Air Development Center

RADC plans and executes research, development, test and selected acquisition programs in support of Command, Control Communications and Intelligence (C^3I) activities. Technical and engineering support within areas of technical competence is provided to ESD Program Offices (POs) and other ESD elements. The principal technical mission areas are communications, electromagnetic guidance and control, surveillance of ground and aerospace objects, intelligence data collection and handling, information system technology, ionospheric propagation, solid state sciences, microwave physics and electronic reliability, maintainability and compatibility.

Printed by
United States Air Force
Hanscom AFB, Mass. 01731